JETIR.ORG ISSN: 2349-5162 | ESTD Year : 2014 | Monthly Issue
JOURNAL OF EMERGING TECHNOLOGIES AND INNOVATIVE RESEARCH (JETIR)
An International Scholarly Open Access, Peer-reviewed, Refereed Journal

STRUCTURAL AND PHOTOLUMINESCENCE PROPERTIES OF Ce^{3+} ACTIVATED $GdPO_4$ PHOSPHORS

[1]Lokeshwar Patel, [2]Manendra Mehta, [3]Rashmi Sharma

[1]Department of Physics, Govt.L.P.P. College, Sarangarh (C.G.), 496445, India

[2]Department of Physics, Govt.E.R.R.PG.Science College, Bilaspur (C.G.),495001, India

[3]Department of Physics, Govt. Aadarsh College, Raipur (C.G.), 492010, India

Abstract

In the present work, Ce^{3+}-activated $GdPO_4$ phosphors were synthesized by the solid-state reaction method. The structural and morphological studies of the synthesized phosphors were characterized by X-ray diffraction (XRD), scanning electron microscopy (SEM), energy dispersive X-ray analysis (EDX), and Fourier-transform infrared (FTIR) spectroscopy. The optical properties of the phosphors were investigated based on the photoluminescence excitation and emission spectra. The results showed that the photoluminescence excitation spectra of $GdPO_4$:Ce^{3+} phosphors were recorded in the range of 300 to 500 nm excited at 512 nm. The PL excitation spectra have two peaks, one peak obtained at 335 nm and the second peak is the most intense peak obtained at 450 nm, which are attributed to the crystal field splitting of Ce^{3+} 4f→5d transition. The excitation peak at 335 nm is attributed to the $^2F_{5/2}$→5D transition and also the peak at 450 nm belongs to $^2F_{7/2}$→5D transitions. In addition to these, the PL emission spectra of these phosphors excited at 430 nm showed a broad emission peak around 557 nm, which is attributed to the transition from the 5d to the 4f energy level. Thus the above result indicates that both the strongest excitation and the strongest emission peak are associated with the lowest-lying 5d state, which is influenced by the crystal field and may be suitable candidates for photonic devices and biomedical applications.

Keywords: $GdPO_4$, solid state reaction method, EDX, FTIR.

1. INTRODUCTION

Recently activated gadolinium orthophosphate ($GdPO_4$) phosphors doped with rare earth ions have attracted researcher attention due to their high band gap, high chemical, and thermal stability, higher quantum yields importantly low toxicity, and bio-compatibility nature [1-2]. These phosphors have outstanding properties of hosting activator ions in their lattice and a high value of magnetic moment (7.94 μB). They have potential applications in many multimodal agents mainly for -state light sources [3], optoelectronic devices [4], light-emitting devices for illumination [5-6], and biomedical applications [2, 7]. Generally, the crystal structure of $GdPO_4$ exhibits two or more two allotropic forms they are in hexagonal, tetragonal, and monoclinic phases. The existence of crystal structure mainly depends upon the synthesis method and conditions such as temperature, reaction medium, and pH parameters [8-10]. It is reported that at low-temperature Eu^{3+} activated $GdPO_4$ crystallizes in the hexagonal form, and at high temperatures, it crystallizes in the monoclinic form [11-13].

Halappa et al prepared the $GdPO_4$ monoclinic phosphors activated with the Series of Eu^{3+} and alkali metal ions (A+ = Li+, Na+, and K+) and investigated their structural parameters. They observed that the intensity of PL emission is enhanced due to mismatches in size and electro-negativity of co-dopant and host cation and magnetic dipole transition ($^5D_0 \rightarrow {}^7F_1$) is higher than the electric dipole transition ($^5D_0 \rightarrow {}^7F_2$). Among all alkali metal ions, Li+ co-doped samples showed higher luminescence intensity, and this phosphor has potential applications in optoelectronic and biomedical fields as it achieves better quantum efficiency, higher lifetime, and excellent chromaticity with high color purity values [14]. Similarly, $GdPO_4$ doped Sm^{3+} phosphate could be an appropriate candidate for display and solid-state lighting applications. These phosphors emit spectra in the reddish-orange region under excitation with 273 nm and 401 nm, which corresponds to the transition of ($^4G_{5/2} \rightarrow {}^6H_J$ = 5/2, 7/2, 9/2, 11/2) Sm^{3+} ion [15]. Another $GdPO_4$:$Tb^{3+,}$ Eu^{3+} nanocrystals reported by Yang et al. [16] which might be a suitable material for the warm-white display field. Under the excitation of 368 nm, the integrated luminescence emission intensity of $GdPO_4$:0.07 Tb^{3+} was approximately 2.62 times stronger in comparison to $GdPO_4 \cdot H_2O$:0.07 Tb^{3+}. Due to the energy transfer mechanism from Tb^{3+} to Eu^{3+} ions the color tone of the phosphor's changes from green and warm white to red color, and by adjusting the concentration unit of Eu^{3+} at 12 mol% and the efficiency of energy transfer reached 96.1%. Several researchers revealed that $GdPO_4$ has been signified as an excellent host lattice for photoluminescence applications [17-18]. Moreover, Ferhi's group prepared $Gd_{(1-x)}Dy_xPO_4$ by simple combustion technique, which could emit blue, yellow, and white light with different concentrations of doped Dy^{3+} [19]. Kumar et al. observed additional excitation/emission channels and multiple energy transfer mechanisms in the $GdPO_4$ host by co-doping Eu^{3+} with the $Yb^{3+,}$ Ho^{3+} pair [20].

In the present work, Ce^{3+} activated $GdPO_4$ phosphor has been synthesized by the solid-state reaction method. The concentration of dopant ions may be varied from 1 to 5 mol%. $GdPO_4$ was chosen as a host matrix due to its good chemical, and thermal stability, low solubility, and specific luminescence properties, and special attention have been given to studying its different characteristics such as XRD, SEM, EDX, PL emission, and TL measurement.

2. EXPERIMENTAL DETAILS

$GdPO_4$ doped with Ce^{3+} phosphors synthesized by the solid-state reaction method. For the synthesis of host material $GdPO_4$, himedia chemicals of gadolinium oxide (Gd_2O_3) and di-ammonium hydrogen phosphate $(NH_4)_2HPO_4$ were used as a starting material. While cerium (III) oxide Ce_2O_3 was used as a dopant source with different concentrations from 1 to 5 mol%. The stoichiometric proportion of all the raw materials was homogeneously mixed and continuously grounded with the help of a mortar pestle. The homogeneous mixture was transferred into the crucible and calcined at 850°c for 8h in a muffle furnace, cooled at room temperature, and again grounded for 5 mins. The resulting product was then used for further characterization. The phase identification and crystal structure of the synthesized powder were evaluated by a PANalytical X'pert Powder X-ray Diffractometer with CuKα radiation of λ= 1.5406 Å. The morphology and elemental analysis of the samples were investigated using a scanning electron microscope and EDX system respectively. Fourier transform infrared spectroscopy (FTIR) studies were carried out to find the nature of the bonding of the phosphors by using potassium bromide (KBr) as a reference sample. The photoluminescence emission and excitation spectra of these samples were recorded through Spectrofluorophotometer. The thermoluminescence (TL) measurements were also investigated temperature using a programmable Nucleonics TL Reader. All the above experimental processes were carried out under ambient conditions.

3. RESULT AND DISCUSSION

3.1 structural characterization

The X-ray diffraction (XRD) pattern of the $GdPO_4$:Ce sample was recorded using a scanning mode for the 2Θ range from 10 to 70° with a scanning step size of 0.02. The diffraction pattern is shown in Fig. 1, which indicates that a sharp intense peak was obtained and matched very well with the JCPDS card no. 84-0920. The crystal structure of prepared $GdPO_4$:Ce is identified as a monoclinic phase with space group P21/n(14) with cell parameters a = 6.65Å, b = 6.85Å, and c = 6.33Å. A small quantity of doping of Ce^{3+} does not affect the crystal structure of $GdPO_4$.

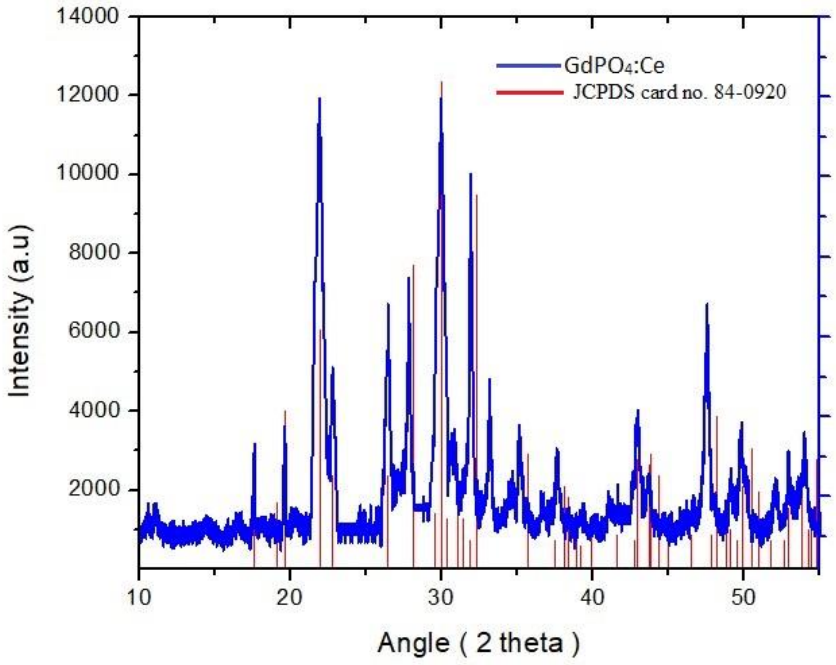

Fig. 1. X ray diffraction (XRD) pattern of $GdPO_4:Ce^{3+}$ phosphors.

3.2 SEM and EDX analysis

Scanning electron microscopy is an important analytical technique to identify the surface morphology and microstructure of crystals. Fig. 2 (a-d) displays the SEM images of undoped and Ce-doped $GdPO_4$. It is observed that the surface morphology of these phosphors is agglomerated and uniform in shape. The particle size distribution is in the order of 5µm. The composition and homogeneity of the phosphor were studied by EDX analysis. The result indicates that the spectra corresponding to the Ce-doped $GdPO_4$ constitute all the major elements. The major elements are gadolinium (Gd), and phosphorus (P). oxygen (O), Cerium (Ce), and along with these elements some traces of impurities in form of carbon was observed. The calculated compositions of various constituent elements present in the prepared $GdPO_4:Ce^{3+}$ phosphors are summarized in Table 1.

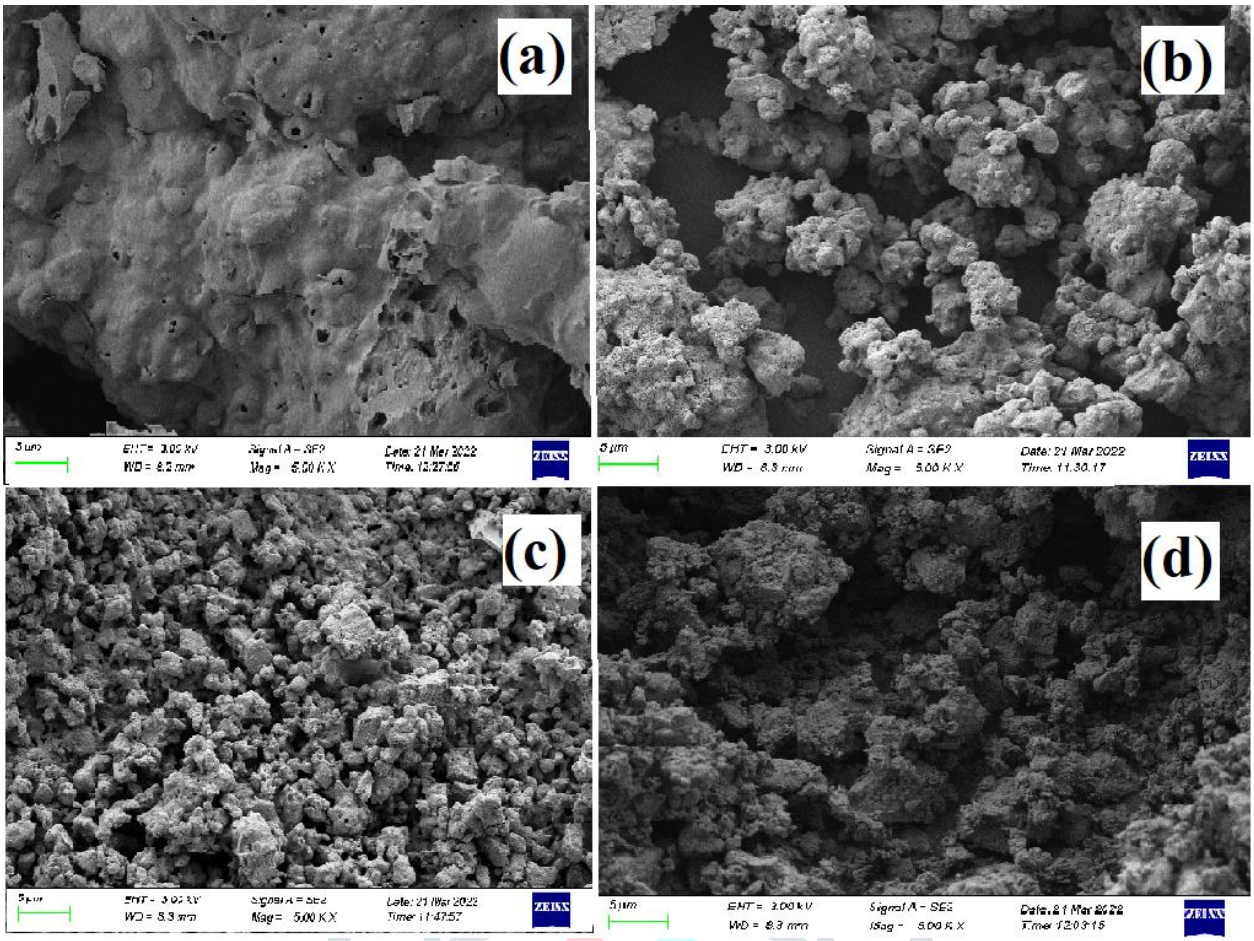

Fig. 2. SEM images of (a) undoped $GdPO_4$ and (b-c) $GdPO_4:Ce^{3+}$(1-3 mol %) phosphors.

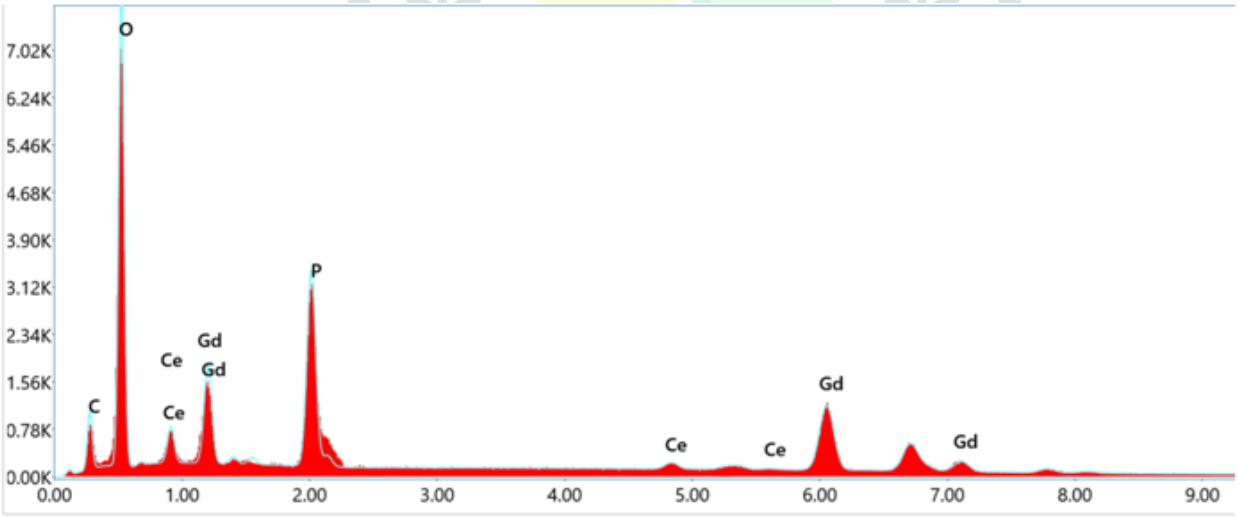

Fig. 3. EDX analysis spectra of $GdPO_4:Ce^{3+}$phosphors

Table 1. Elemental composition of $GdPO_4:Ce^{3+}$ phosphors

S.No.	Elements	Weight %	Atomic %
1	C K	15.4	34.3
2	O K	29.6	49.6
3	P K	9.5	8.2
4	Ce L	2.4	0.5
5	Gd L	43.1	7.4
	Total	**100.00**	**100.00**

3.3 Fourier Transforms Infrared spectroscopy (FTIR) spectroscopy

The confirmation of the phase purity and the molecular vibration of phosphate-based phosphor were analyzed through FTIR spectra in the frequency range from 400 to 1800 cm^{-1} as earlier discussed in the literature [21]. The recorded spectra of the $GdPO_4:Ce^{3+}$ are shown in Fig. 4. The band obtained in the region between 400 to 800 cm^{-1} was ascribed to the bending vibrations of the PO^{4-} tetrahedron. The band observed at 554 to 800 cm^{-1} can be ascribed to the asymmetric bending vibrations of P-O bonds and a weak band at 464 cm^{-1} arises due to the symmetric bending vibrations mode. The band obtained at around 900 t0 1235 cm^{-1} region can be assigned to the stretching mode of PO_4^{3-} tetrahedron. Other than above mentioned peaks, no additional peak were obtained in the FTIR spectra, which confirm the presence of functional group and phase purity of the phosphate-based phosphors [22-25].

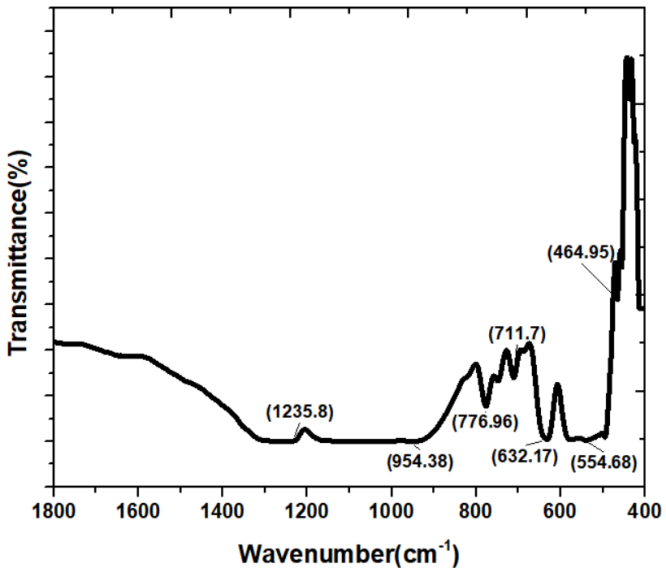

Fig. 4. FTIR spectra of GdPO4:Ce^{3+}phosphors.

3.4 Photoluminescence properties

The photoluminescence excitation and emission spectra of the synthesized powder for varying concentrations of Ce^{3+} were depicted in Fig. 5 and Fig. 6. Ce^{3+} ion has the simplest configuration of a one-electron system. The electronic configuration of Ce^{3+} in the ground state and the excited state are $4f^1$ and $5d^1$, respectively. The ^4F_j ground state of $^4f_1$ is split into $^2F_{7/2}$, and $^2F_{5/2}$, and the ^2D_J excited state is split into $^2D_{3/2}$, and $^2D_{5/2}$ states due to spin-orbit interaction. Since the radial wave function of the ^2D_J excited state of $^5d_1$ electron extends spatially well beyond the closed $5s^25p^6$, their states are strongly much more influenced by crystal field interaction [26- 27]. The excitation spectra of $GdPO_4:Ce^{3+}$ phosphors are reported in the range of 300 to 500 nm. At 512 nm emission wavelength, the PL excitation spectra have two peaks, one peak at 335 nm and the second peak is the most intense peak obtained at 450 nm, which are attributed to the crystal field splitting of Ce^{3+} 4f-5d transition. The maximum intensity was observed for 4 mol% Ce^{3+} concentration. The excitation peak at 335 nm is attributed to the $^2F_{5/2}\rightarrow$5D transition and also the peak at 450 nm belongs to $^2F_{7/2}\rightarrow$5D transitions [28]. The PL emission spectra of $GdPO_4:Ce^{3+}$ phosphor excited at

430 nm were measured in the wavelength range from 450 to 600 nm. One broad emission peak is observed near 557 nm, which is attributed to the transition from the 5d to the 4f energy level. Therefore, both the strongest excitation and the strongest emission peak are associated with the lowest-lying 5d state and are influenced by the crystal field [29].

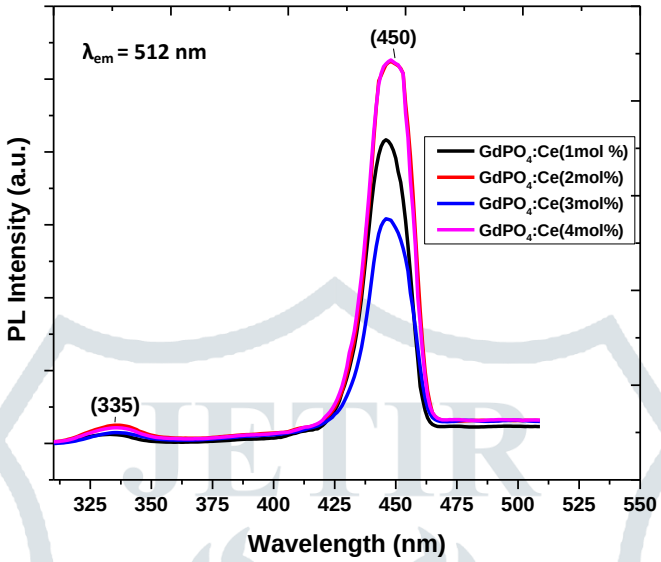

Fig. 5. PL excitation spectra of $GdPO_4:Ce^{3+}$ phosphors.

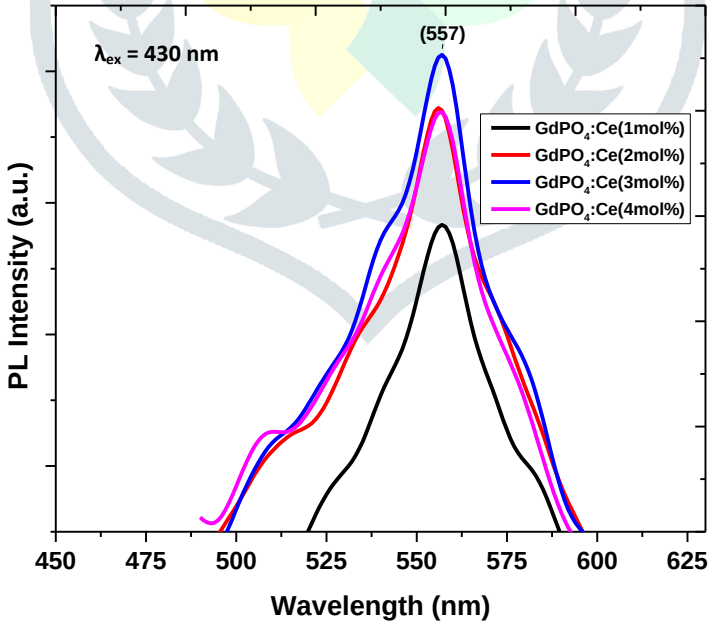

Fig. 6. PL emission spectra of $GdPO_4:Ce^{3+}$ phosphors monitored at λ_{ex} = 430 nm.

4. Conclusions

$GdPO_4:Ce^{3+}$ phosphors have been successfully synthesized by solid-state reaction method with a varying concentration ranging from 1 to 5 mol%. The structural, surface morphology, and elemental composition of synthesized phosphor were investigated by the XRD, scanning electron microscopy (SEM), and energy dispersive X-ray analysis (EDX) respectively. The XRD pattern confirmed that these phosphors enclose a

monoclinic phase with space group P21/n(14) with cell parameters a = 6.65Å, b = 6.85Å, and c = 6.33Å. The SEM micrographs showed the surface morphology of these phosphors is agglomerated, and uniform in shape, and the average particle size distribution is in the order of 5µm. The EDX result indicates that the spectra corresponding to the Ce-doped $GdPO_4$ constitute the major elements gadolinium (Gd), and phosphorus (P). oxygen (O), Cerium (Ce), and along with these elements some traces of impurities in form of carbon was observed. The FTIR analysis confirmed the presence of a functional group and good phase purity of the phosphate-based phosphors. The optical behavior of the synthesized phosphor was investigated in form of photoluminescence. The PL excitation spectra revealed that these phosphors exhibit two characteristic peaks, one at 335 nm and the second peak is the most intense peak obtained at 450 nm, which are attributed to the crystal field splitting of the Ce^{3+} 4f-5d transition. The PL emission spectra consist of a single broad emission peak centered at 557 nm, which is attributed to the transition from the 5d to the 4f energy level. The investigated results indicate that the synthesized phosphor could be a potential candidate for solid-state lighting and biomedical applications.

References:

[1] L. Zhang, M. Yin, H. You, M. Yang, Y. Song, Y. Huang, 2011. Multifunctional $GdPO_4:Eu^{3+}$ Hollow Spheres: Synthesis and Magnetic and Luminescent Properties, Inorg. Chem. 50, 10608–10613.
[2] J. Cho, C.H. Kim, 2014. Solid-state phase transformation mechanism from hexagonal $GdPO_4$: Eu^{3+} nanorods to monoclinic nanoparticles, RSC Adv. 4, 31385–31392.
[3] N.K. Sahu, N.S. Singh, L. Pradhan, D. Bahadur, 2014. Ce^{3+} sensitized $GdPO_4:Tb^{3+}$ with iron oxide nanoparticles: a potential biphasic system for cancer theranostics, Dalton. Trans. 43, 11728–11738.
[4] Z. Yi, W. Lu, C. Qian, T. Zeng, L. Yin, H. Wang, 2014. Urchin-like Ce/Tb co-doped $GdPO_4$ hollow spheres for in vivo luminescence/X-ray bio-imaging and drug delivery, Biomater. Sci.2, 1404–1411.
[5] S. Rodriguez-Liviano, A.I. Becerro, D. Alcantara, V. Grazu, J.M. de la Fuente, M. Ocana, 2013. Synthesis and properties of multifunctional tetragonal Eu: $GdPO_4$ nanocubes for optical and magnetic resonance imaging applications, Inorg. Chem. 52, 647–654.
[6] V. Kumar, P. Rani, D. Singh, S. Chawla, 2014. Efficient multiphoton upconversion and synthesis route dependent emission tunability in GdPO4:$Ho^{3+,}$ Yb^{3+} nanocrystals, RSC Adv. 4, 36101–36105.
[7] J. Huang, Z. Lv, Y. Wang, Z. Wang, T. Gao, N. Zhang, M. Guo, H. Zou, P. Zhang, 2016. In Vivo MRI and X-Ray Bifunctional Imaging of Polymeric Composite Supplemented with 24 $GdPO_3$, ·HO Nanobundles for Tracing Bone Implant and Bone Regeneration, Adv. Healthcare Mater. 5, 2182-2190.
[8] S.R. Liviano, A.I. Becerro, D. Alcantara, V. Grazu, J.M. de la Fuente, M. Ocaña, 2013. Synthesis and properties of multifunctional tetragonal Eu: $GdPO_4$ nanocubes for optical and magnetic resonance imaging applications, Inorg. Chem. 52, 647–654.
[9] Y.P. Fang, A.W. Xu, R.Q. Song, H.X. Zhang, L.P. You, J.C. Yu, H.Q. Liu, 2003. Systematic synthesis and characterization of single-crystal lanthanide orthophosphate nano-wires, J. Am. Chem. Soc. 125, 16025–16034.
[10] Y.W. Zhang, Z.G. Yan, L.P. You, R. Si, C.H. Yan, 2003. General Synthesis and Characterization of Monocrystalline Lanthanide Orthophosphate Nanowires, Eur. J. Inorg. Chem. 4099–4104.
[11] N.K. Sahu , R.S. Ningthoujam, D. Bahadur, 2012. Disappearance and recovery of luminescence in $GdPO_4:Eu^{3+}$nanorods: Propose to water/OH• release under near infrared and gamma irradiations, J. Appl. Phys. 112, 014306-014317.
[12] H. Lai, X. Yang, H. Yang, 2012. Luminescent properties of $GdPO_4$: Eu nanorods, J. Mater. Sci.: Mater. Electron. 23, 285-289.
[13] M.A.Hassairi, A.Garrido Hernández, T.Kallel, M.Dammak, D.Zambon, G.Chadeyron, A.Potdevin, D.Boyer, R.Mahiou, 2016. Spectroscopic properties and Judd–Ofelt analysis of Eu^{3+}doped $GdPO_4$ nanoparticles and nanowires, J. Lumin. 170, 200–206.
[14] P. Halappa, A. Mathur, D. Marie-Heleneץ and C. Shivakumara. 2018. Alkali metal ion co-doped Eu^{3+} activated $GdPO_4$ phosphors: Structure and photoluminescence properties. Journal of Alloys and Compounds 740 DOI: 10.1016/j.jallcom.2018.01.087
[15] G. Ouertani, M. Ferhi, K. Horchani-Naifer, & M. Ferid, 2021. Effect of Sm^{3+} concentration and excitation wavelength on spectroscopic properties of $GdPO_4:Sm^{3+}$ phosphor. Journal of Alloys and Compounds, 885, 161178. doi:10.1016/j.jallcom.2021.161178 .

[16] J. Yang, X. Wang, L. Song, N. Luo, J. Dong, S. Gan, L. Zou, 2018. Tunable luminescence and energy transfer properties of $GdPO_4:Tb^{3+,}$ Eu^{3+} nanocrystals for warm-white LEDs. Optical Materials, 71–78. doi:10.1016/j.optmat.2018.08.043

[17] J.F. Yang, H.L. Xiong, J.C. Dong, C.M. Yang, S.C. Gan, L.C. Zou, 2017. Facile hydrothermal synthesis and luminescent properties of Sm^{3+} /Eu^{3+} codoped $GdPO_4$ phosphors, J. Phys. Chem. Solid. 111, 355–363.

[18] S. Goderski, M. Runowski, N. Stopikowska, S. Lis, 2017. Luminescent-plasmonic effects in $GdPO_4$: Eu^{3+} nanorods covered with silver nanoparticles, J. Lumin. 188, 24–30.

[19] M. Ferhi, S. Toumi, K.H. Naifer, M. Ferid, 2017. Single phase $GdPO_4$: Dy^{3+} microspheres blue, yellow and white light emitting phosphor, J. Alloy. Comp. 714, 144–153.

[20] V. Kumar, G.F. Wang, 2018. Tuning green-to-red ratio of Ho^{3+} /Yb^{3+} activated $GdPO_4$ upconversion luminescence through Eu 3+ doping, J. Lumin. 199, 188–193.

[21] J. Heuser, A. Bukaemskiy, S. Neumeier, A. Neumann, D. Bosbach, 2014. Raman and infrared spectroscopy of monazite-type ceramics used for nuclear waste conditioning, Progress in Nuclear Energy, 72, 149-155.

[22] M. Ferhi, K.H. Naifer, M. Fe´rid, 2009. Combustion synthesis and luminescence properties of LaP: Eu (5%), J. Rare Earths. 27, 182-186.

[23] K. Nakamoto, 1986. Infrared and Raman Spectra of Inorganic and Coordination Compounds. 5th ed., New York, Wiley, USA,

[24] E. N. Silva, A. P. Ayala, I. Guedes, C. W. A. Paschoal, R. L. Moreira, C. K. Loong, L.A.Boatner, 2006. Vibrational spectra of monazite-type rare-earth orthophosphates, Optical Materials, 29, 2–3, 224-230.

[25] A. A. Ansari, J. P. Labis and M. Aslam Manthrammel, 2017. Designing of luminescent $GdPO_4$: Eu@ $LaPO_4$@ SiO_2 core/shell nanorods: Synthesis, structural and luminescence properties, Solid State Sciences, 71, 117-122.

[26] Z. Xia, A. Meijerink A. 2017. Ce^{3+} doped garnet phosphors: composition modi□cation, luminescence properties and applications. Chem Soc Rev. 46:275–299.

[27] A. Singh, S. Arya, M. Khanuja, et al. 2020. Eu doped $NaYF_4$ @Er: TiO_2 nanoparticles □or tunable ultraviolelight based anti-counter□eiting applications. Microsyst Technol. 1–10. https://doi.org/10.1007/s00542-019-04734-3

[28] A. Katelnikovas, J. Plewa, D. Dutczak, S. Möller, D. Enseling, H. Winkler, A. Kareiva, T. Jüstel, 2012. Opt. Mater. 34, 1195.

[29] L. Chen, C.C. Lin, C.W. Yeh, R.S. Liu, 2010. Materials 3, 2172.